A Modulator-Free Photonic Triangular Pulse Generator Based on Semiconductor Lasers

Pei Zhou, *Student Member, IEEE*, Fangzheng Zhang, *Member, IEEE*, Qingshui Guo, and Shilong Pan, *Senior Member, IEEE*

***Abstract*— A modulator-free photonic triangular pulse generator is proposed and demonstrated based on two semiconductor lasers. In this method, a direct-modulated semiconductor laser is employed to generate a fundamental frequency component. Meanwhile, a third-order harmonic signal is generated by external optical injection together with 1/3 subharmonic microwave modulation of another semiconductor laser. After properly setting the amplitude and time delay between the fundamental and third-order harmonics, the combined signal composes a triangular waveform. The generation of a 11.4-GHz triangular pulse train is experimentally demonstrated. Without using any modulator, the proposed approach is a promising method for triangular pulse generation with low cost and simple structure.**

***Index Terms*— Semiconductor laser, microwave photonics, triangular pulse generation, optical injection.**

I. Introduction

PHOTONIC generation of triangular-shaped waveform has attracted increasing interest because of its wide applications in optical signal processing and manipulation, such as all-optical frequency conversion, doubling of optical pulses, optical pulse compression, as well as signal copying [1], [2]. Up to now, numerous photonic approaches have been proposed to generate triangular pulses [3]–[10]. Among these schemes, one method is using spectral shaping followed by frequency-to-time mapping (FTTM) [3]. In such system, the optical spectrum of a mode-locked laser is shaped by an optical spectral shaper (e.g., a spatial light modulator). Then, FTTM is performed through a dispersive element to generate triangular pulses in time domain. Main drawback of these schemes is that the use of ultra-short pulses and spatial light modulator leads to a high cost. Besides, the generated triangular pulse usually has a small duty cycle (<1). Nevertheless, triangular pulses with full-duty-cycle are more preferred for many applications [1]. Fortunately, the method based on external modulation of a continuous wave (CW) light can generate full-duty-cycle triangular pulses [4]–[10]. In these systems, the triangular pulses are usually obtained by generating a 1st-order harmonic and a 3rd-order harmonic with an amplitude ratio of nine, of which the combination composes a triangular waveform in time domain. For example, in [4], a dual-drive Mach-Zehnder modulator (MZM) and a section of dispersion fiber are used to generate triangular pulses. In this setup, the dispersive fiber is used to suppress unwanted harmonics. A single-drive MZM can also be used to generate triangular pulses. In [5], a MZM is first biased at minimum-transmission-point (MITP). Then, optical spectral processing including stimulated Brillouin scattering (SBS) -based carrier recovery and optical filtering are followed to generate triangular pulses. In order to remove the additional optical devices (such as a dispersion fiber or an optical filter) in [4] and [5], photonic generation of triangular pulses using a single dual-parallel MZM has been proposed [6], [7]. But two RF signals with different frequencies [6] or a RF 90-degree hybrid [7] are required. Besides, a single dual-polarization modulator can also be applied to generate triangular pulses [8]. A common problem with these schemes is that the use of electro-optical modulators increases the system cost and suffers from the bias drifting problem.

In this letter, we propose and experimentally demonstrate an approach to generate triangular pulses using two semiconductor lasers driven by a single-frequency RF signal. In this method, a semiconductor laser is first direct-modulated to obtain the fundamental frequency component. Meanwhile, external optical injection drives another semiconductor laser to period-one (P1) nonlinear dynamics of which the oscillation frequency can be tuned to be 3 times of the fundamental frequency, and then the same RF signal is applied to stabilize the P1 oscillation frequency. Therefore, the desired 3rd-order harmonic signal can be obtained with other harmonics well suppressed. After properly setting the amplitude and time delay, the two signals are synthesized to generate a triangular pulse train. To the best of our knowledge, this is the first modulator-free photonic triangular pulse generator, which can greatly reduce the system cost and complexity.

II. Principle

Figure 1 shows the schematic diagram of the proposed photonic triangular pulse generator. The key devices in the scheme are two commercial semiconductor lasers, i.e., SL1 and SL2. A sinusoidal signal with frequency f_m is split into two parts. In the upper branch, a continuous wave (CW) light from a tunable laser source (TLS) is injected to SL1 through an optical circulator. To maximize the injection efficiency, the

Manuscript received April 16, 2018; revised May 26, 2018; accepted June 5, 2018. Date of publication June 11, 2018; date of current version June 27, 2018. This work was supported by the Fundamental Research Funds for the Central Universities under Grant NS2018028. *(Corresponding authors: Fangzheng Zhang; Shilong Pan.)*

The authors are with the Key Laboratory of Radar Imaging and Microwave Photonics, Ministry of Education, Nanjing University of Aeronautics and Astronautics, Nanjing 210016, China (e-mail: zhangfangzheng@nuaa.edu.cn; pans@ieee.org).

Color versions of one or more of the figures in this letter are available online at http://ieeexplore.ieee.org.

Digital Object Identifier 10.1109/LPT.2018.2845850

1041-1135 © 2018 IEEE. Personal use is permitted, but republication/redistribution requires IEEE permission.
See http://www.ieee.org/publications_standards/publications/rights/index.html for more information.

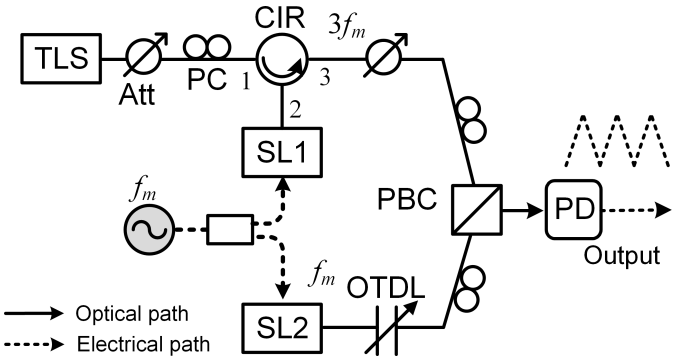

Fig. 1. Schematic diagram of the proposed photonic triangular pulse generator. TLS: tunable laser source; Att: optical attenuator; PC, polarization controller; CIR: optical circulator; SL: semiconductor laser; OTDL: optical tunable delay-line; PBC: polarization beam combiner; PD, photodetector.

polarization of the injection light and SL1 are matched through a polarization controller before the optical circulator. After proper optical injection, SL1 can operate at the P1 oscillation state by undamping the relaxation resonance [11]. The output intensity of the injected SL1 shows self-sustained intensity oscillation with frequency f_o. By varying the injection strength and/or the detuning frequency, the P1 frequency f_o can be tuned from a few to over a hundred gigahertz [12]. Here, the injection strength is defined as the square root of the power ratio between the injected light and the free-running slave laser. In our scheme, the P1 frequency f_o is tuned to be 3 times of the fundamental frequency, i.e., $f_o = 3f_m$. However, the generated 3rd-order harmonic signal through P1 dynamics suffers from a relatively large linewidth, which is on the order of megahertz. In order to stabilize the P1 oscillation, an external subharmonic microwave modulation technique is utilized [13]. A portion of the sinusoidal signal f_m is applied to modulate SL1 and linewidth of the generated $3f_m$ signal can be significantly reduced through 1/3 subharmonic microwave modulation. In the lower branch, SL2 is direct-modulated by the sinusoidal signal to obtain the fundamental frequency component. After properly setting the amplitudes and time delay between the two branches through an optical attenuator and a tunable optical delay-line, the generated frequency components at f_m and $3f_m$ are combined and synthesized to generate desired waveform in the following polarization beam combiner (PBC) and photodetector (PD). If the frequency components at f_m and $3f_m$ have an amplitude ratio of 9:1, the output electrical signal after PD can be expressed as

$$S(t) \propto DC + \cos(2\pi f_m t) + \frac{1}{9}\cos(3 \times 2\pi f_m t) \qquad (1)$$

which corresponds to an approximate form of a triangular pulse train with frequency f_m.

III. Experiment Results

An experiment is carried out to verify the feasibility of the proposed method based on the setup in Fig. 1. The semiconductor lasers (SL1 and SL2) are commercial DFB lasers (Actech LD15DM). SL1 is biased at 45.6 mA, of which the free-running wavelength and power are 1544.748 nm and 7.15 dBm, respectively. SL2 is biased at 44.9 mA, and its

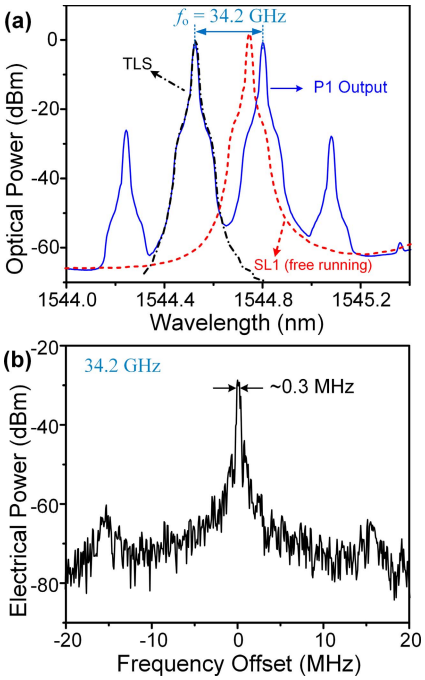

Fig. 2. (a) Optical spectra of the injection light (black), the free-running SL1 (red), and the injected SL1 (blue) when injection strength equals to 0.9. (b) Electrical spectrum of the generated 34.2 GHz signal. RBW = 100 kHz.

output wavelength and power are 1544.012 nm and 7.17 dBm. A sinusoidal signal from a microwave signal generator (Agilent E8257D) is divided into two parts by an electrical coupler. An optical tunable delay-line (OTDL, General Photonics Inc.) with a tuning range of 600 ps is used to match the time delay between the two branches. At the optical output, a 50-GHz PD (u2t XPDV2120RA) is used to implement optical-to-electrical conversion. Temporal waveform of the generated triangular pulse train is observed through an 80-GHz sampling oscilloscope (OSC, Agilent 86100A). Electrical spectral properties are measured by an electrical spectral analyzer (ESA, R&S FSWP50), and the optical spectrum is monitored by an optical spectrum analyzer (OSA, Yokogawa AQ6370C).

First of all, the electrical driving signal f_m is not applied to SL1. The wavelength of the TLS is set to be 1544.526 nm, corresponding to a master-slave detuning frequency of 27.8 GHz. The injection strength to SL1 is varied by adjusting the optical attenuator. The optical spectrum of P1 dynamics is measured at port 3 of optical circulator and the result is shown in Fig. 2(a) (blue curve) when the injection strength equals to 0.9. For comparison, optical spectra of the injection light (black curve) and the free-running SL1 (red curve) are also shown in Fig. 2(a). As can be seen, two highly dominant wavelength components separated by a P1 oscillation frequency of 34.2 GHz is observed after optical injection. To verify the quality of the generated electrical signal after photodetection, the electrical spectrum is also measured. Due to the intrinsic laser noise, a relatively broad 3-dB linewidth of 0.3 MHz is observed in Fig. 2(b), which hardly meets the requirement in triangular pulse generation. Then the electrical driving signal with frequency f_m of 11.4 GHz and power

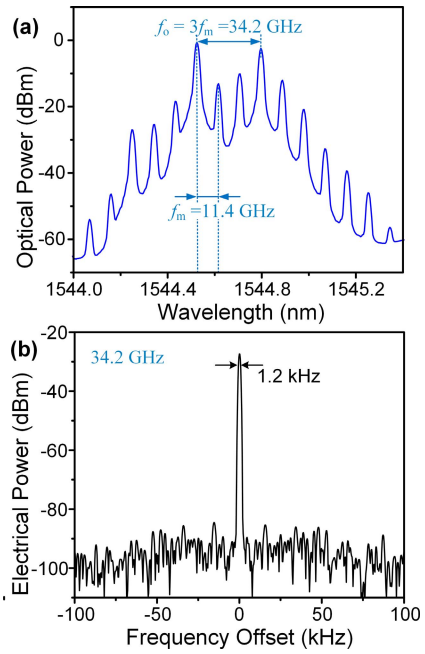

Fig. 3. (a) Optical spectrum of the injected SL1 with 1/3 subharmonic microwave modulation. (b) Electrical spectrum of the generated 34.2 GHz signal. RBW = 1 kHz.

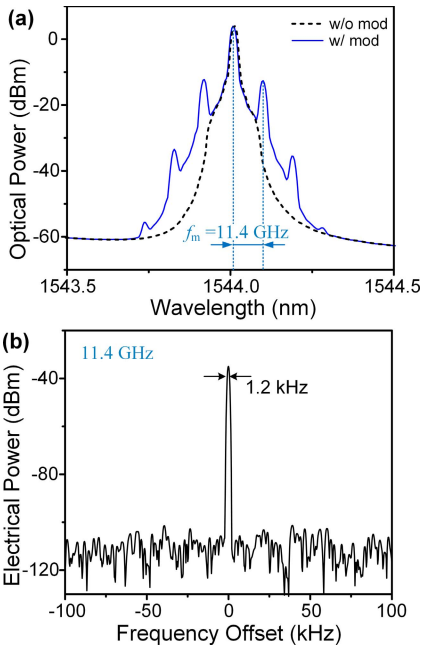

Fig. 4. (a) Optical spectra of SL2 with (blue) and without modulation (black). (b) Electrical spectrum of the generated 11.4 GHz signal. RBW = 1 kHz.

of 18 dBm is applied to modulate SL1. Figure 3(a) shows the resultant optical spectrum of the injected SL1 when 1/3 subharmonic microwave modulation is adopted. As can be observed in Fig. 3(a), frequency difference between the two strongest peaks remains to be 34.2 GHz, which is equal to $3f_m$. Meanwhile, the sidebands of direct modulation with frequency f_m also exist. Thanks to the 1/3 subharmonic microwave modulation, the generated microwave signal is stably locked with a much smaller linewidth. As shown in Fig. 3(b), the 3-dB linewidth of the 34.2 GHz signal is reduced to 1.2 kHz.

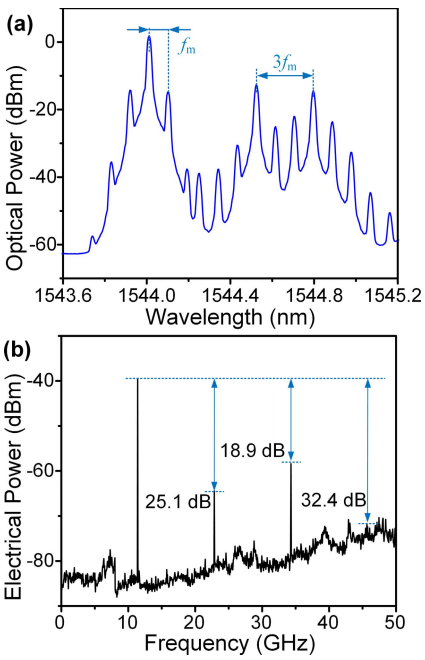

Fig. 5. (a) Optical and (b) electrical spectrum of the generated 11.4 GHz triangular pulse train. RBW = 100 kHz.

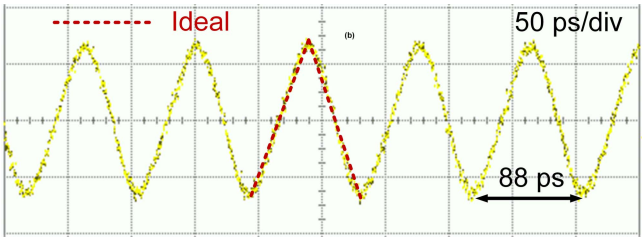

Fig. 6. Measured waveform of the 11.4-GHz triangular pulse train.

In the lower branch, a portion of the electrical driving signal f_m is applied to modulate SL2. Figure 4(a) shows the optical spectra of SL2 with (blue curve) and without modulation (black curve). After photodetection, a 11.4-GHz signal is obtained, of which the 3-dB linewidth is measured to be 1.2 kHz, as shown in Fig. 4(b).

After properly setting the amplitude and time delay between the two branches, the generated frequency components at f_m and $3f_m$ are combined and synthesized to generate a triangular pulse train after the PBC and PD. Here, a tunable delay-line is used to match the time delay. The amplitude ratio can be controlled by an optical attenuator and/or the PCs before PBC. Utilization of a PBC also makes the optical signals in the two branches orthogonally polarized. Furthermore, considering that the optical carriers have different wavelengths in each branch, the influence of optical interference between the two branches can be eliminated. Figure 5(a) is the optical spectrum of the generated 11.4-GHz triangular pulse train which is measured at the output of PBC. The electrical triangular pulse train is obtained after the PD. Figure 5(b) shows the electrical spectrum. It can be seen that the third-order harmonic at 34.2 GHz is 18.9 dB lower than the fundamental component, which is very close to the ideal value of 19.08 dB (corresponding to an amplitude ratio of 1/9). In this case, temporal waveform of the 11.4-GHz triangular pulse train is measured by the

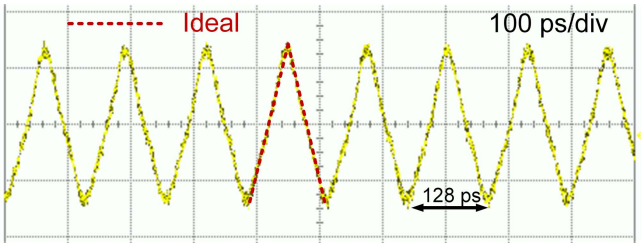

Fig. 7. Measured waveform of the 7.8-GHz triangular pulse train.

oscilloscope. As shown in Fig. 6, the obtained waveform shows a good consistency with an ideal triangular pulse train. The root-mean-square error (RMSE) is calculated to be 4.07e-2, which is comparable to the results in [9] and [10]. It should be noted that, although the waveform is already very close to a triangular waveform, its quality can be further improved by suppressing the undesired harmonic components. In Fig. 5(b), the fourth-order harmonic is 32.4 dB lower than the fundamental component, and the second-order harmonic, which is generated by modulation of SL1, is 25.1 dB lower than the fundamental component. To reduce the second-order harmonic, one can cascade another semiconductor laser in the upper branch for frequency selecting by injection locking [14].

The tunability of the proposed system is also investigated. By changing the electrical driving signal f_{m} and P1 oscillation frequency of SL1, the repetition rate of the obtained triangular pulse train can be tuned. Figure 7 shows the result when the system is configured to generate a 7.8-GHz triangular pulse train. It can be seen that the measured waveform is also very close to an ideal triangular pulse train. In the experiment, the available repetition rate of the generated triangular pulse train is mainly restricted by the modulation bandwidth of SL2, which is around 10 GHz. By replacing SL2 with a high-speed semiconductor laser [15], the tunability of our approach could be further enlarged.

IV. Discussion and Conclusion

It should be noted that, the delay and power ratio variations between the two branches may affect the quality of generated waveform. Compared to an ideal synthesized waveform based on Eq. (1), when the delay mismatch varies within ± 0.6 ps (for an 11.4-GHz triangular pulse train), or the power ratio between f_{m} and $3f_{\mathrm{m}}$ components varies in the range of 18.05-20.26 dB, the RMSE of the generated triangular waveform can be controlled to be less than 0.01. In our experiment, after properly setting the amplitude and time delay, the obtained triangular waveform is stable within an observation period of 20 minutes and the corresponding RMSEs are also stable.

In conclusion, we have proposed and experimentally demonstrated a modulator-free photonic triangular pulse generator based on semiconductor lasers. The triangular pulse is obtained by synthesizing the f_{m} and $3f_{\mathrm{m}}$ components. In the system, the f_{m} component is generated by direct modulation of SL2, while the $3f_{\mathrm{m}}$ component is obtained by P1 oscillation of SL1. In the experiment, triangular pulse trains with repetition rates of 7.8 GHz and 11.4-GHz are successfully generated, which fits well with the ideal waveforms. Without using any modulator, the proposed approach is more promising because of its low cost and simple structure.

References

[1] A. I. Latkin, S. Boscolo, R. S. Bhamber, and S. K. Turitsyn, "Optical frequency conversion, pulse compression and signal copying using triangular pulses," in *Proc. 34th Eur. Conf. Opt. Commun.*, Brussels, Belgium, Sep. 2008, pp. 1–2.

[2] N. Verscheure and C. Finot, "Pulse doubling and wavelength conversion through triangular nonlinear pulse reshaping," *Electron. Lett.*, vol. 47, no. 21, pp. 1194–1196, 2011.

[3] J. Ye *et al.*, "Photonic generation of triangular-shaped pulses based on frequency-to-time conversion," *Opt. Lett.*, vol. 36, no. 8, pp. 1458–1460, Apr. 2011.

[4] J. Li, X. Zhang, B. Hraimel, T. Ning, L. Pei, and K. Wu, "Performance analysis of a photonic-assisted periodic triangular-shaped pulses generator," *J. Lightw. Technol.*, vol. 30, no. 11, pp. 1617–1624, Jun. 1, 2012.

[5] X. Liu *et al.*, "Photonic generation of triangular-shaped microwave pulses using SBS-based optical carrier processing," *J. Lightw. Technol.*, vol. 32, no. 20, pp. 3797–3802, Oct. 15, 2014.

[6] J. Li *et al.*, "Photonic generation of triangular waveform signals by using a dual-parallel Mach–Zehnder modulator," *Opt. Lett.*, vol. 36, no. 19, pp. 3828–3830, Oct. 2011.

[7] F. Zhang, X. Ge, and S. Pan, "Triangular pulse generation using a dual-parallel Mach–Zehnder modulator driven by a single-frequency radio frequency signal," *Opt. Lett.*, vol. 38, no. 21, pp. 4491–4493, Nov. 2013.

[8] F. Zhang, B. Gao, and S. Pan, "Time-domain waveform synthesis using a dual-polarization modulator," *IEEE Photon. Technol. Lett.*, vol. 28, no. 23, pp. 2689–2692, Dec. 1, 2016.

[9] W. Y. Wang, W. Li, W. H. Sun, W. Wang, J. G. Liu, and N. H. Zhu, "Triangular microwave waveforms generation based on an opto-electronic oscillator," *IEEE Photon. Technol. Lett.*, vol. 27, no. 5, pp. 522–525, Mar. 1, 2015.

[10] Y. Gao, A. Wen, H. Zheng, D. Liang, and L. Lin, "Photonic microwave waveform generation based on phase modulation and tunable dispersion," *Opt. Exp.*, vol. 24, no. 12, pp. 12524–12533, Jun. 2016.

[11] T. B. Simpson, J. M. Liu, K. F. Huang, and K. Tai, "Nonlinear dynamics induced by external optical injection in semiconductor lasers," *J. Eur. Opt. Soc. B, Quantum Semiclass Opt.*, vol. 9, no. 5, pp. 765–784, May 1997.

[12] P. Zhou, F. Zhang, Q. Guo, S. Li, and S. Pan, "Reconfigurable radar waveform generation based on an optically injected semiconductor laser," *IEEE J. Sel. Topics Quantum Electron.*, vol. 23, no. 6, Nov./Dec. 2017, Art. no. 1801109.

[13] L. Fan *et al.*, "Subharmonic microwave modulation stabilization of tunable photonic microwave generated by period-one nonlinear dynamics of an optically injected semiconductor laser," *J. Lightw. Technol.*, vol. 32, no. 23, pp. 4058–4064, Dec. 1, 2014.

[14] D. S. Wu, R. Slavik, G. Marra, and D. J. Richardson, "Direct selection and amplification of individual narrowly spaced optical comb modes via injection locking: Design and characterization," *J. Lightw. Technol.*, vol. 31, no. 14, pp. 2287–2295, Jul. 15, 2013.

[15] Y. Matsui *et al.*, "55-GHz bandwidth short-cavity distributed reflector laser and its application to 112-Gb/s PAM-4," in *Proc. Opt. Fiber Commun. Conf.*, Mar. 2016, pp. 1–3.